JℳRAPIDS

On the attainable metastability of liquids during depressurisation – effect of pre-existing bubbles

Alexandra Metallinou Log (ORCID)

SINTEF Energy Research, P.O. Box 4761 Torgarden, NO-7465 Trondheim, Norway
Corresponding author: Alexandra Metallinou Log, alexandra.log@sintef.no

The attainable metastability is key to the behaviour of liquids undergoing rapid depressurisation. This tells us how far the liquid can be depressurised, or stretched, before phase change occurs. Previous work on the depressurisation of liquids through nozzles and pipes shows that classical nucleation theory (CNT) can predict the attainable metastability close to the critical point, but fails at lower temperatures. In the latter case, it is common to correct the CNT prediction using a strongly temperature-dependent empirical reduction factor. In the present work, we show that the trend at low temperatures naturally follows if the metastability of the liquid is limited by the growth of pre-existing bubbles. With the new volume balancing method, we calculate the attainable metastability for systems with pre-existing bubbles and attain excellent fit with data for both CO_2 and water systems. The method has one tuning parameter related to the number of available bubbles in the flow, which is temperature independent.

Key words: compressible flows, boiling, phase change

1. Introduction and background

The depressurisation of liquids and subsequent phase change from liquid to gas (known as flashing or flash boiling) has broad industrial relevance. Applications range from ejectors in refrigeration systems (Angielczyk *et al.* 2010; Banasiak & Hafner 2013; Ringstad *et al.* 2020; Wilhelmsen & Aasen 2022) to cryogenic propellants in spacecrafts (Hendricks *et al.* 1972, 1976; Lyras *et al.* 2021; Weber & Dreyer 2023), safety estimates for nuclear cooling systems (Edwards & O'Brien 1970; Lienhard, Alamgir & Trela 1978; Alamgir, Kan & Lienhard 1980; Alamgir & Lienhard 1981; Barták 1990; Deligiannis & Cleaver 1990; Bartosiewicz & Seynhaeve 2014) and CO_2 transportation networks (Botros *et al.* 2016; Munkejord *et al.* 2020; Hammer *et al.* 2022; Log *et al.* 2024a). For a slow process, flashing
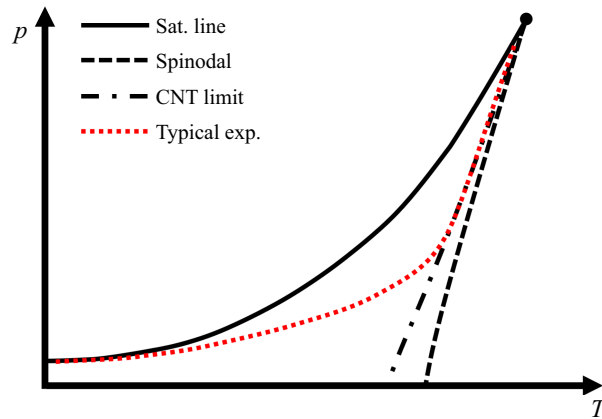
Figure 1. Example phase diagram showing the typical trend for the attainable metastability found in experiments for depressurising liquids. Here, p denotes pressure and T denotes temperature.

will occur at the saturation pressure. However, for rapid depressurisation, the phase change often occurs delayed, at a lower pressure than the saturation pressure, where the liquid is metastable.

The formation and growth of bubbles has a significant impact on the resulting mass flow, pressure and temperature in the system. It is therefore key to understand the attainable metastability for the liquid: How metastable can the liquid become? When will the phase change start affecting the flow? Several experimental campaigns have been conducted on this topic for different fluids and industrial systems (Edwards & O'Brien 1970; Hendricks *et al.* 1972, 1976; Lienhard *et al.* 1978; Alamgir *et al.* 1980; Barták 1990; Banasiak & Hafner 2013; Haida *et al.* 2018; Hammer *et al.* 2022; Log *et al.* 2024*a*). The experimental data show the following overall trend: for high reduced temperature and pressure, the attained metastability during depressurisation agrees well with the limit predicted by classical nucleation theory (CNT). However, at lower reduced temperature and pressure there is a gradual deviation from CNT until the experimental results agree with the saturation line instead. A drawing illustrating the trend is shown in figure 1.

Classical nucleation theory is based on the assumption that a new phase will form in a mother phase due to random thermal density fluctuations (Debenedetti 1997). For the case of bubbles forming in a liquid, the density fluctuations in the liquid (caused by random movement of the molecules) can create some lower density areas that are large enough for stable bubbles to form and grow. This process occurs throughout the fluid and is denoted as homogeneous nucleation.

Based on statistical physics, and some simplifying assumptions, the rate of creation of critically sized bubbles during homogeneous nucleation can be calculated. The rate takes the following form (Debenedetti 1997):

$$J_{hom} = K \exp\left(-\frac{E_B}{k_B T}\right), \tag{1.1}$$

where K is a kinetic prefactor, E_B is the energy barrier of the bubble formation, and $k_B T$ is the available energy for the bubbles to form; k_B is the Boltzmann constant and T is the liquid temperature. The rate of creation of stable bubbles is much stronger near the critical point (where the density difference between the liquid and gas phases is small) and for high temperatures (where the density fluctuations are bigger).

In order to make the nucleation theory fit to data from depressurisation experiments at lower temperatures, it is common to introduce a reduction factor ϕ for the energy required to nucleate a bubble (Alamgir & Lienhard 1981; Barták 1990; Deligiannis & Cleaver 1992; Elias & Chambré 1993; Banasiak & Hafner 2013; Wilhelmsen & Aasen 2022). The factor ϕ is intended to represent the reduction of energy required to nucleate a bubble on a surface as opposed to nucleating in the bulk of the liquid. Theoretical derivations of ϕ exist for nucleation on a surface (heterogeneous nucleation), accounting for the contact angle of the bubble, and an idealised surface geometry (Wilt 1986; Debenedetti 1997). However, the theoretical derivations do not agree with the experimental data.

Researchers have fitted and applied a reduction factor on CNT for their depressurisation data and prediction of metastability since at least the 1970s (Lienhard *et al.* 1978), and the practice is still used today (Banasiak & Hafner 2013; Wilhelmsen & Aasen 2022). The reduction factor is found to be a function of the reduced temperature of the liquid, and the depressurisation rate, i.e., how quickly the pressure is reduced in the system (Alamgir & Lienhard 1981; Barták 1990; Deligiannis & Cleaver 1992; Elias & Chambré 1993). More specifically, ϕ decreases exponentially for lower reduced temperatures and pressures. For water tests, reduction factors smaller than 10^{-6} are found. This begs the question: Why would the energy barrier for bubbles forming through density fluctuations be over six orders of magnitude smaller than that predicted by CNT at low temperatures? Perhaps the bubbles in these experiments are not forming through density fluctuations.

Classical nucleation theory is based on idealised systems. In real systems, surfaces are rough and have imperfections. Small crevices and cavities on a surface may be non-wetted, i.e., containing trapped gas bubbles (Bankoff 1958; Hsu 1962; Apfel 1970; Atchley & Prosperetti 1989; Collier & Thome 1994; Chappell & Payne 2007). The presence of such bubbles is well established, and necessary to explain boiling caused by heat transfer in real systems. Pre-existing bubbles lower the required heat needed for bubbles to grow and be released (Collier & Thome 1994). This effect can be observed when boiling water on the stove at home. Bubbles tend to form and rise from specific spots in the pot where small imperfections on the pot's surface have trapped bubbles. Some attempts have been made to describe the attainable metastability of liquids during depressurisation based on bubbles trapped in cavities (Lee & Schrock 1990; Xu, Chen & Chen 1997). These models focus on describing the pressure at which bubbles start advancing from the cavities, the point at which evaporation into them can begin. However, they still require strong temperature-dependent fitting, suggesting that there is a temperature-dependent effect which the models do not include.

If an ample amount of pre-existing bubbles are available on the system surface, evaporation into them will inevitably begin at some point during depressurisation. The volume created during evaporation is strongly temperature dependent. At lower pressures and temperatures, the specific volume of the gas phase increases significantly, causing significant volume creation during evaporation. We therefore suggest that the missing temperature-dependent effect is volume creation from the evaporation itself.

In the present work, we introduce the novel volume balancing method for calculating the attainable metastability during depressurisation of a liquid. The method is based on the assumption that pre-existing bubbles are present in the flow, and the calculation is straightforward and intuitive: balancing the rate of volume loss caused by outflow from the system with the rate of volume creation from evaporation into the available bubbles.

The remainder of the paper is structured as follows. We introduce the equations applied to calculate the attainable metastability of liquids during depressurisation in § 2. The method is compared with experimental data for CO_2 and water in § 3, and a summary and conclusion are provided in § 4.

Figure 2. Overview of the concept behind the volume balancing method. The attainable metastability is found at the pressure where the volume loss out of the system is balanced by the bubble growth inside the system.

2. The volume balancing method

2.1. *Concept*

It is well known that real systems have imperfect surfaces, and small pits and crevices on the surfaces can lead to pre-existing gas bubbles being present in a liquid-filled container (Bankoff 1958; Hsu 1962; Apfel 1970; Atchley & Prosperetti 1989; Collier & Thome 1994; Chappell & Payne 2007). Furthermore, during the depressurisation of a liquid, the pressure must keep decreasing unless the volume lost by the liquid outflow is somehow replaced.

Based on this knowledge, we propose the following.

(i) The attainable metastability for depressurising liquids in real systems is not limited by the nucleation rate of bubbles, but by the evaporation rate into existing ones.
(ii) The limit occurs at the pressure where the rate of volume loss of liquid caused by the outflow from the system is balanced by the rate of volume creation caused by evaporation/bubble growth.

This allows us to formulate the volume balancing method for predicting the limit of metastability for liquid depressurisation with pre-existing bubbles:

$$\dot{V}_{loss} = \dot{V}_{growth}, \tag{2.1}$$

where $\dot{V}_{loss}$ denotes the volume loss rate of the system and $\dot{V}_{growth}$ denotes the volume creation rate caused by evaporation into existing bubbles. This equality only holds at a short moment at the point where the metastability limit is reached.

The basis of the volume balancing method is illustrated in figure 2. The bubbles in the flow stem from pre-existing gas trapped on imperfections on the system's surface. The derivations of the volume loss caused by the liquid outflow and the volume creation due to bubble growth are provided below.

2.2. *Liquid outflow*

Consider a constant-area pipe being depressurised, such that a rarefaction wave is moving into the pipe. We consider a control volume which encompasses the entire rarefaction wave marked with dashed lines in figure 2. To the left of the control volume, the fluid is at its initial condition with pressure p_0, entropy s_0 and flow speed $u_0 = 0$. To the right of the control volume, the pressure of the fluid has reduced to pressure, p, and the flow has reached a speed u. The volume loss rate from the system caused by the outflow is

$$\dot{V}_{loss} = (u - u_0)A = uA, \tag{2.2}$$

where A is the cross-sectional area of the pipe.

In a rarefaction wave, the following invariants hold:

$$s = \text{const.}, \quad dp + \rho c \, du = 0, \tag{2.3}$$

where ρ is the density and c the speed of sound of the fluid. The invariants can be found through manipulations of the Euler equations for inviscid flows (LeVeque 2002,

see § 14.10). Since the entropy is constant, we can determine the flow speed at a given pressure as

$$u(p, p_0, s_0) = \int_{p_0}^{p} \frac{1}{\rho(p', s_0)c(p', s_0)} \mathrm{d}p'. \tag{2.4}$$

Rarefaction waves are self-similar in time, so (2.4) holds at any given time, t. The only difference is how far the wave has stretched, i.e., the length of our control volume.

2.3. *Bubble growth*

The volume creation rate due to bubble growth can be expressed as

$$\dot{V}_{growth} = 4\pi r_{bub}^2 \dot{r}_{bub} n_{bub}, \tag{2.5}$$

where r_{bub} is the mean bubble radius and n_{bub} denotes the number of bubbles growing in the control volume. n_{bub} is treated as a tuning parameter in the model, and is chosen to fit experimental data.

The mean radius of the bubbles is here modelled using the asymptotic solution of the well-established model of Plesset & Zwick (1954). This describes the radius of a growing bubble limited by heat transfer to its surface (Collier & Thome 1994) (a simple formula for inertia-controlled bubble growth was also tested, but using this relation did not recover the trends seen in experimental data):

$$r_{bub} = \frac{2\Delta T_{sat} k_l}{h_{l,g}\rho_g} \left(\frac{3t}{\pi d_l} \right)^{1/2}. \tag{2.6}$$

Here, $d_l(p, s_0)$ is the thermal diffusivity of the liquid, $k_l(p, s_0)$ is its thermal conductivity, $h_{l,g}(p, s_0)$ the latent heat of evaporation, $\Delta T_{sat} = T_l(p, s_0) - T_{sat}(p)$ is the liquid superheat, and t is the time the bubble has been growing. h_k denotes the specific enthalpy of phase k, gas is denotes with subscript g and liquid with subscript l. The asymptotic solution (2.6) was derived under the assumption that the bubble wall temperature has fallen to the saturation temperature $T_{sat}(p)$ (Collier & Thome 1994).

We set the time for bubble growth to $t = 10^{-4}$ s. This value is chosen as it is representative for the time scales where pressure measurements from depressurisation experiments start showing signs of bubbles affecting the flow (Edwards & O'Brien 1970; Lienhard *et al.* 1978; Barták 1990; Log *et al.* 2024*a* (Increased time for bubble growth, e.g., due to a slower decompression would lead to a higher volume creation rate and lower attained metastability. This is in agreement with experimental results from various sources, e.g., Lienhard & Lienhard (1984); Barták (1990); Elias & Chambré (1993); Log *et al.* (2024*a*))).

Note that r_{bub} is calculated as if the pressure, p, where the bubbles are growing remained constant over the time t. This is a simplification, as we are considering a depressurising system. As n_{bub} is a tuning parameter, it can compensate to some extent for errors introduced by the assumptions and simplifications made in the method. The present formulation is sufficient to illustrate the effect of pre-existing bubbles on the attainable metastability in a depressurising liquid. More precise equations can be considered in further work, both to describe the volume loss and the bubble growth.

2.4. *Solution method*

With the expressions for the rate of volume loss and the rate of volume creation introduced above, the following equation must be solved for the limiting pressure p_{lim} to determine
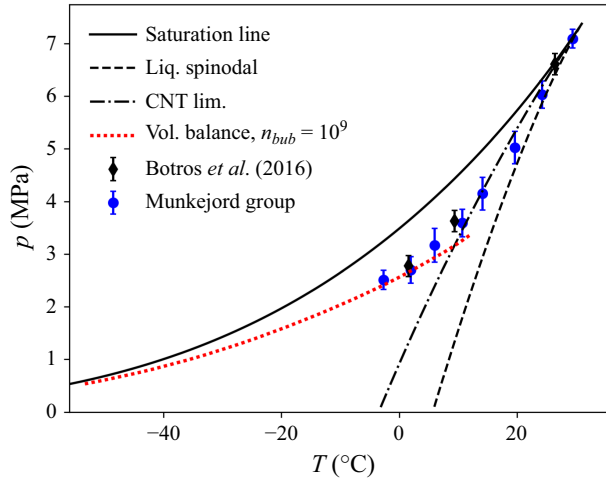
Figure 3. The attainable metastability calculated with the volume balancing method for $n_{bub} = 10^9$, and the attained metastability from the CO_2 pipe depressurisation tests of Botros *et al.* (2016) and the Munkejord group (Munkejord *et al.* 2020; Log *et al.* 2024*a*,*b*).

the attainable metastability of the system at the given entropy s_0 and initial pressure p_0:

$$\dot{V}_{loss}(p_{lim}, p_0, s_0) = \dot{V}_{growth}(p_{lim}, s_0). \tag{2.7}$$

In the present work, the integral in (2.4) is evaluated numerically using the trapezoidal rule. The thermodynamic variables are evaluated using SINTEF's in-house version of the thermodynamic library Thermopack (Wilhelmsen *et al.* 2017). The upper integration limit, p, in (2.4) is incremented until $\dot{V}_{growth}(p, p_0, s_0) \geqslant \dot{V}_{loss}(p, s_0)$, at which point the limiting pressure $p_{lim} = p$ has been identified. An example calculation script is uploaded at Log (2025).

The calculation is conducted for a range of initial temperatures (providing a range of initial entropies), such that the predicted metastability limit for depressurisation can be mapped in the phase diagram. The resulting limit is compared with experimental data, and n_{bub} is adjusted to fit the observations.

3. Results

In the following, the volume balancing method is applied to estimate the attainable metastability of liquid CO_2 and water during depressurisation. For calculations with CO_2, the Span & Wagner (1996) equation of state is applied. For calculations with water, the IAPWS (Wagner & Pruß 2002) equation of state is applied. Remarkably, we find that n_{bub} can be kept constant for a given system and fluid. It is not a function of the system's pressure or temperature. This marks a significant improvement over the conventional energy barrier reduction factor applied with CNT-based methods, with its orders-of-magnitude variation with temperature.

3.1. *Comparison with CO_2 experiments*

Several pipe depressurisation experiments have been conducted for CO_2 to assess the safety of CO_2 transport pipelines. For such tests, the pressure sensor mounted closest to the open end of the pipe tends to show significant attained metastability of the liquid phase.
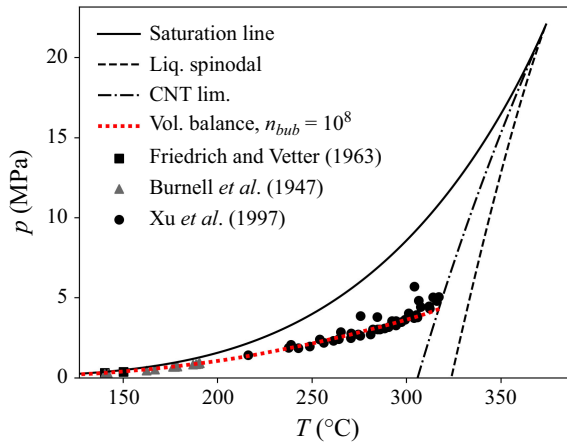
Figure 4. The attainable metastability calculated with the volume balancing method for $n_{bub} = 10^8$, and experimental water depressurisation tests from Burnell (1947), Friedrich & Vetter (1962) and Xu *et al.* (1997).

The volume balancing method shows good agreement with the trend of the experimental results from Botros *et al.* (2016) and the Munkejord group (Munkejord *et al.* 2020; Log *et al.* 2024*a*,*b*) with $n_{bub} = 10^9$. This is shown in figure 3. For the calculation, p_0 was set to 12 MPa, which agrees with most of the tests by the Munkejord group.

The volume balancing method reproduces the typical trend of lower attainable metastability at low reduced temperatures and pressures. This is due to the volume creation from bubble growth being much stronger in this region, as the specific volume for the gas phase is very large compared with the liquid phase. More experimental data at colder conditions would be needed to verify the trend for CO_2.

3.2. *Comparison with water experiments*

There have been significantly more tests conducted for rapid depressurisation of water. Wilhelmsen & Aasen (2022) estimated the onset of flash boiling for water based on the experimental data of Burnell (1947), Friedrich & Vetter (1962) and Xu *et al.* (1997). We find excellent agreement with these data for the volume balancing method using $n_{bub} = 10^8$, as shown in figure 4. Here, $p_0 = 40$ MPa was selected to reproduce the high depressurisation rates in the experiments, as many were conducted in converging–diverging nozzles. Once again, the trend in the attainable metastability is reproduced due to the large specific volume of the gas phase at low reduced pressures and temperatures.

3.3. *Sensitivity to the tuning parameter, n_{bub}*

We apply one tuning parameter, n_{bub}, in the volume balancing method. To assess the method's sensitivity to n_{bub}, the predicted metastability limit of water with pre-existing bubbles is shown in figure 5 for $n_{bub} \in [10^5, 10^{12}]$. We observe that the predicted metastability limit remains in qualitative agreement with experimentally observed trends across the range of n_{bub} values. At low reduced temperatures and pressures, the attainable metastability is relatively insensitive to the choice of n_{bub} since the limit is any case close to the saturation line. At higher temperatures and pressures, the sensitivity increases. These observations suggest that, for a given system, n_{bub} can be tuned using a single measurement of p_{lim} at an appropriate temperature. As a rule of thumb, measuring p_{lim}
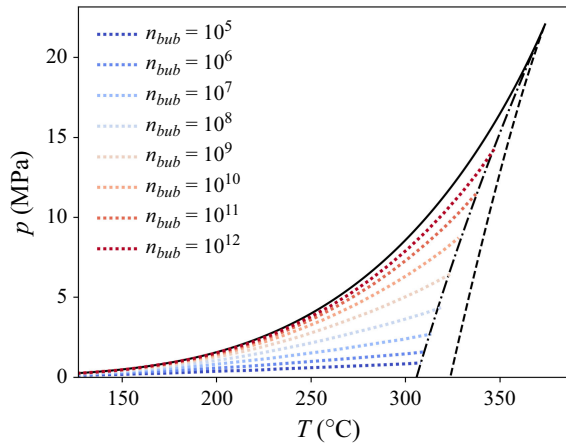
Figure 5. The attainable metastability for water calculated with the volume balancing method with various choices of the tuning parameter, n_{bub}.

at the temperature for which CNT predicts $p_{CNT\,\text{lim}} = 0\,\text{Pa}$ should yield a good estimate for n_{bub}.

4. Summary and conclusion

The present work suggests that the attainable metastability of depressurising liquids in real systems at low reduced temperatures is not limited by the nucleation of bubbles, but by evaporation into existing ones. The limiting pressure can be estimated by balancing the volume creation from evaporation into pre-existing bubbles on the system's surface, with the volume loss from depressurisation-driven outflow. We denote this the volume balancing method. The method shows good agreement with experimental data from CO_2 and water depressurisation tests, despite having only a single, temperature-independent tuning parameter. This marks a significant improvement compared with the orders-of-magnitude temperature dependence of the tuning parameters in previously published models, typically based on CNT. Possible future work includes evaluating the model for additional systems and fluids, improving on simplifications made in the model to improve the interpretability of the tuning parameter, and investigating possibilities of determining the parameter *a priori*.

REFERENCES

ALAMGIR, MD, KAN, C.Y. & LIENHARD, J.H. 1980 An experimental study of the rapid depressurization of hot water. *J. Heat Transfer* **102** (3), 433–438.

ALAMGIR, M. & LIENHARD, J.H. 1981 Correlation of pressure undershoot during hot-water depressurization. *J. Heat Transfer* **103** (1), 52–55.

ANGIELCZYK, W., BARTOSIEWICZ, Y., BUTRYMOWICZ, D. & SEYNHAEVE, J.-M. 2010 1-D modeling of supersonic carbon dioxide two-phase flow through ejector motive nozzle. In International Refrigeration and Air Conditioning Conference. Purdue University.

APFEL R.E. 1970 The role of impurities in cavitation-threshold determination. *J. Acoust. Soc. Am.* **48**, 1179–1186.

ATCHLEY A.A. & PROSPERETTI A. 1989 The crevice model of bubble nucleation. *J. Acoust. Soc. Am.* **86**, 1065–1084.

BANASIAK, K. & HAFNER, A. 2013 Mathematical modelling of supersonic two-phase R744 flows through converging–diverging nozzles: the effects of phase transition models. *Appl. Therm. Engng* **51** (1), 635–643.

BANKOFF, S.G. 1958 Entrapment of gas in the spreading of a liquid over a rough surface. *AIChE J.* **4**, 24–26.

BARTÁK, J. 1990 A study of the rapid depressurization of hot water and the dynamics of vapour bubble generation in superheated water. *Intl J. Multiphase Flow* **16**, 789–798.

BARTOSIEWICZ, Y. & SEYNHAEVE, J.-M. 2014 Delayed equilibrium model (DEM) of flashing choked flows relevant to LOCA and implementation in system codes. In Proceedings of the 2014 22nd International Conference on Nuclear Engineering, vol. 2B: Thermal Hydraulics, pp. V02BT09A040. ASME.

BOTROS, K.K., GEERLIGS, J., ROTHWELL, B. & ROBINSON, T. 2016 Measurements of decompression wave speed in pure carbon dioxide and comparison with predictions by equation of state. *Trans ASME: J. Press. Vessel Technol.* **138** (3), 031302.

BURNELL, J. 1947 Flow of boiling water through nozzles, orifices and pipes. *Engineering* **164**, 572–576.

CHAPPELL M.A. & PAYNE S.J. 2007 The effect of cavity geometry on the nucleation of bubbles from cavities. *J. Acoust. Soc. Am.* **121**, 853–862.

COLLIER, J.G. & THOME, J.R. 1994 *Convective Boiling and Condensation*, 3rd edn. Oxford University Press.

DEBENEDETTI, P.G. 1997 *Metastable Liquids: Concepts and Principles*. Princeton University Press.

DELIGIANNIS, P. & CLEAVER, J.W. 1990 The role of nucleation in the initial phases of a rapid depressurization of a subcooled liquid. *Intl J. Multiphase Flow* **16** (6), 975–984.

DELIGIANNIS, P. & CLEAVER, J.W. 1992 Determination of the heterogeneous nucleation factor during a transient liquid expansion. *Intl J. Multiphase Flow* **18** (2), 273–278.

EDWARDS, A.R. & O'BRIEN, T.P. 1970 Studies of phenomena connected with the depressurization of water reactors. *J. British Nucl. Energy Soc.* **9** (2), 125–135.

ELIAS, E. & CHAMBRÉ, P.L. 1993 Flashing inception in water during rapid decompression. *J. Heat Transfer* **115** (1), 231–238.

FRIEDRICH, H. & VETTER, G. 1962 Influence of nozzle shape on the through flow behavior of jets for water at various thermodynamic states. *Energy* **14**, 3.

HAIDA, M., SMOLKA, J., HAFNER, A., PALACZ, M., BANASIAK, K. & NOWAK, A.J. 2018 Modified homogeneous relaxation model for the r744 trans-critical flow in a two-phase ejector. *Intl J. Refrig.* **85**, 314–333.

HAMMER, M., DENG, H., AUSTEGARD, A., LOG, A.M. & MUNKEJORD, S.T. 2022 Experiments and modelling of choked flow of CO_2 in orifices and nozzles. *Intl J. Multiphase Flow* **156**, 104201.

HENDRICKS, R.C., SIMONEAU, R.J. & BARROWS, R.F. 1976 Two-phase choked flow of subcooled oxygen and nitrogen. Technical Note NASA TN D-8169. National Aeronautics and Space Administration (NASA).

HENDRICKS, R.C., SIMONEAU, R.J. & EHLERS, R.C. 1972 Choked flow of fluid nitrogen with emphasis on the thermodynamic critical region. Technical Memorandum TM X-68107. National Aeronautics and Space Administration (NASA).

HSU, Y.Y. 1962 On the size range of active nucleation cavities on a heating surface. *J. Heat Transfer* **84** (3), 207–213.

LEE, S.Y. & SCHROCK, V.E. 1990 Critical two-phase flow in pipes for subcooled stagnation states with a cavity flooding incipient flashing model. *J. Heat Transfer* **112** (4), 1032–1040.

LEVEQUE, R.J. 2002 *Finite Volume Methods for Hyperbolic Problems*. Cambridge University Press.

LIENHARD, J.H., ALAMGIR, M. & TRELA, M. 1978 Early response of hot water to sudden release from high pressure. *Trans. ASME: J. Heat Transfer* **100** (3), 473–479.

J.H. LIENHARDV & J.H. LIENHARD(IV) 1984 Velocity coefficients for free jets from sharp-edged orifices. *J. Fluids Engng* **106** (1), 13–17.

LOG, A.M. 2025 Calculate metastability limit for liquid depressurization using volume balancing method. https://gist.github.com/alexanml/c19140d2e0c3b2385a3723ebc99ef64f

LOG, A.M., HAMMER, M., DENG, H., AUSTEGARD, A., HAFNER, A. & MUNKEJORD, S.T. 2024*a* Depressurization of CO_2 in pipes: effect of initial state on non-equilibrium two-phase flow. *Intl J. Multiphase Flow* **170**, 104624.

LOG, A.M., HAMMER, M. & MUNKEJORD, S.T. 2024*b* A flashing flow model for the rapid depressurization of CO_2 in a pipe accounting for bubble nucleation and growth. *Intl J. Multiphase Flow* **171**, 104666.

LYRAS, T., KARATHANASSIS, I.K., KYRIAZIS, N., KOUKOUVINIS, P. & GAVAISES, M. 2021 Modelling of liquid oxygen nozzle flows under subcritical and supercritical pressure conditions. *Intl J. Heat Mass Transfer* **177**, 121559.

MUNKEJORD, S.T., AUSTEGARD, A., DENG, H., HAMMER, M., STANG, H.G.J. & LØVSETH, S.W. 2020 Depressurization of CO_2 in a pipe: high-resolution pressure and temperature data and comparison with model predictions. *Energy* **211**, 118560.

PLESSET, M.S. & ZWICK, S.A. 1954 The growth of vapor bubbles in superheated liquids. *J. Appl. Phys.* **25** (4), 493–500.

RINGSTAD, K.E., ALLOUCHE, Y., GULLO, P., ERVIK, Å., BANASIAK, K. & HAFNER, A. 2020 A detailed review on CO_2 two-phase ejector flow modeling. *Therm. Sci. Engng Prog.* **20**, 100647.

SPAN R. & WAGNER W. 1996 A new equation of state for carbon dioxide covering the fluid region from the triple-point temperature to 1100 K at pressures up to 800 MPa. *J. Phys. Chem. Ref. Data* **25** (6), 1509–1596.

WAGNER, W. & PRUß, A. 2002 The IAPWS formulation 1995 for the thermodynamic properties of ordinary water substance for general and scientific use. *J. Phys. Chem. Ref. Data* **31** (2), 387–535.

WEBER, N.H. & DREYER, M.E. 2023 Depressurization induced vapor bubble growth in liquid methane during microgravity. *Cryogenics* **134**, 103716.

WILHELMSEN, Ø. & AASEN, A. 2022 Choked liquid flow in nozzles: crossover from heterogeneous to homogeneous cavitation and insensitivity to depressurization rate. *Chem. Engng Sci.* **248**, 117176.

WILHELMSEN, Ø., AASEN, A., SKAUGEN, G., AURSAND, P., AUSTEGARD, A., AURSAND, E., GJENNESTAD, M.A., LUND, H., LINGA, G. & HAMMER, M. 2017 Thermodynamic modeling with equations of state: present challenges with established methods. *Ind. Engng Chem. Res.* **56** (13), 3503–3515.

WILT, P.M. 1986 Nucleation rates and bubble stability in water-carbon dioxide solutions. *J. Colloid Interface Sci.* **112** (2), 530–538.

XU, J.L., CHEN, T.K. & CHEN, X.J. 1997 Critical flow in convergent-divergent nozzles with cavity nucleation model. *Expl Therm. Fluid Sci.* **14**, 166–173.